Reaction Enthalpy and Reaction Volume Changes upon Photoenolization: 2-Methylbenzophenone

Masahide Terazima

Department of Chemistry, Graduate School of Science, Kyoto University, Kyoto, 606, Japan

Received: August 21, 1997; In Final Form: October 29, 1997

The transient grating (TG) signal after photoexcitation of 2-methylbenzophenone is fully analyzed in detail in terms of the thermal contribution by the nonradiative transition from the excited states, enthalpy change (ΔH) by the photoisomerization from the *cis*- and *trans*-enol forms to the keto form, molecular volume change (ΔV) by the reaction, and population grating contribution due to the absorption change. From a quantitative measurement of the TG intensity combined with that of the photoacoustic intensity, ΔH and ΔV are determined simultaneously without changing any external properties such as solvents, pressure or temperature. The intermolecular hydrogen bonding species (*trans*-enol) diffuses more slowly than the keto form, which provides clear evidence of the enol formation. The molecular volume of the enol form is smaller than that of the keto form, and the contraction is explained by the intermolecular hydrogen bonding. The obtained physical quantities, ΔH, ΔV, and diffusion constant of the keto and enol forms, are discussed relating to the molecular structure.

1. Introduction

After photoexcitation of a molecule, the created excited states relax to the ground state radiatively or nonradiatively, or they could relax to form a new species by a chemical reaction. Photophysical properties (such as lifetimes and energies of the excited states, quantum yields of radiative or nonradiative transitions) as well as photochemical properties of the excited states (such as a quantum yield of a reaction, enthalpy change (ΔH), volume change (ΔV)) are important to characterize or to understand chemical reactions.[1−3] Measurements of photophysical properties have been one of the main subjects for a long time and have been carried out by various techniques which have been developed extensively with the aid of laser technology. On the other hand, experimental techniques for measurements of ΔH and ΔV have been rather limited. Traditionally, temperature dependence and pressure dependence of a reaction rate or an equilibrium constant have been analyzed to determine these quantities.[1−3] However, for irreversible fast reactions, these conventional techniques are difficult to use. Alternatively, photoacoustic (PA) spectroscopy, which detects the pressure wave created by the reaction has been applied to that purpose.[4−7] There are two limitations, however, in this method. First, the thermal contribution (ΔH) and the volume contribution (ΔV) are always mixed in the signal and separating them is not trivial. Generally, the efficiency of the pressure wave generation by the thermal expansion is varied to isolate the thermal contribution. This variation can be achieved either by using the temperature dependence of dn/dT of aqueous solution or by changing solvents. Always we have to assume that the chemical reaction itself (quantum yield, ΔH or ΔV) does not depend on these properties. We cannot apply this technique to a reaction which is sensitive to the matrix or temperature. Second, the time window of the PA signal is limited in a rather narrow range. If the reaction proceeds in a time scale out of this window, the PA method cannot provide any kinetic information.

A similar measurement is possible using the thermal lens (TL),[8] the beam deflection,[9] or a pressure wave detection by the transient grating (TG) method.[10,11] The TG is created when molecules in a solution are excited by two laser beams, which are overlapped in space within their coherence time and the acoustic wave is detected as the diffraction of a probe beam. Although the TL, beam deflection, or TG method can trace the temporal development of the chemistry continuously after the photoexcitation on a long time scale, the contribution of the volume and thermal energy should be separated by a similar manner as the PA method. There are some disadvantages or limitations in this separation method as discussed previously.[8]

As another approach, recently we presented a new TG method to separate the contribution of the thermal energy from the volume effect so that we could determine ΔH and ΔV simultaneously including the temporal evolution.[8,12] In this TG method, the separation of the volume and thermal effects is achieved on the basis of different rates between the thermal diffusion and species (mass) diffusion. This method does not require any modulation of external properties such as solvent, temperature, or pressure, and many difficulties in the conventional methods can be eliminated. We have applied this technique to photodissociation reactions of diphenylcyclopropanone (DPCP)[8,12] and diazo compounds,[13] and also trans−cis isomerization of azobenzenes.[14] The chemical reactions we have examined so far complete in a initial stage of the TG signal, even faster than the pulse width of the excitation laser we used. However, considering a high time resolution of the TG method, we should be able to continuously monitor the time evolution of ΔH and ΔV after the excitation.

In this study, as a demonstration of the time-resolved TG technique for a more complex (time evoluting, solvent sensitive, and more than two products) reaction, we apply this TG method to the measurement of ΔH and ΔV upon photoenolization of 2-methylbenzophenone (MBP) from submicrosecond to 10's milliseconds time range. After photoexcitation of MBP, intramolecular hydrogen transfer takes place in the lowest excited triplet (T_1) state efficiently (quantum yield $\sim$ 1 in ethanol) and yields the 1,4-biradical (Scheme 1).[15−17] The biradical forms

S1089-5639(97)02726-6 CCC: $15.00
Published on Web 01/15/1998

SCHEME 1

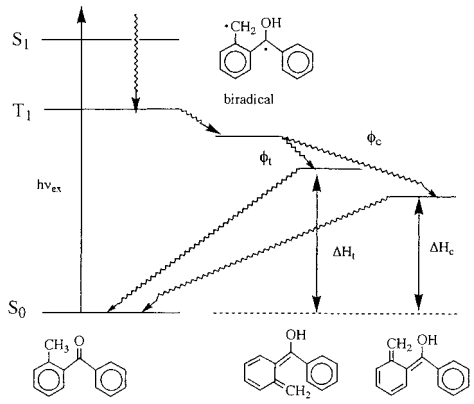

trans- and *cis*-enol forms within 26 ns. The *cis*-enol decays back to the keto form by the back hydrogen transfer with a lifetime about 4 μs. The trans form survives on a few milliseconds time scale (the lifetime $\sim$ 5.8 ms from the transient absorption measurement[17]). Recently, Suzuki et al. first applied a photothermal method (thermal lens) to this system and analyzed the signal in terms of the energies of the cis and trans forms.[17] They determined the energy of the *trans*-enol (202 kJ/mol) and *cis*-enol (116 kJ/mol). The energy difference of 86 kJ/mol was attributed to the structural hindrance. However, their analysis was limited only to the energetic consideration. Possible volume change and contribution of the population lens signal, which are difficult to be evaluated by the thermal lens technique, were neglected. Here we fully analyze the TG signal after the photoexcitation of MBP in terms of the thermal energy by nonradiative transition from the excited state, ΔH, ΔV, and the population grating component. The grating signal clearly indicates a large contribution of the species grating besides the thermal effect. The result shows that the volume effect and the population effect should be adequately treated in the TG or TL analysis. The determined quantities are discussed based on the molecular structural change by the photoenolization.

2. Experimental Section

The TG setup has been described previously.[18] Briefly, the third harmonic of a Nd:YAG laser (Spectra-Physics GCR-170) was split into two by a beam splitter and crossed inside a quartz sample cell (optical path length = 1 cm). The laser power of the excitation was $\leq$10 μJ/pulse. The created interference pattern (transient grating) in the sample was probed by a He−Ne laser as a Bragg diffracted signal (TG signal). The TG signal was detected by a photomultiplier (Hamamatsu R928) and averaged by a digital oscilloscope. The photoacoustic signal was detected by a piezoelectric transducer (PZT) as described previously.[19] The signal was directly detected by the digital oscilloscope and averaged about 100 times. The repetition rate of the excitation laser was about 3 Hz, and the sample was gently stirred during the measurement to prevent possible excitation of photoproduct (enol form). The sample was deaerated by the nitrogen bubbling method. All measurements were carried out at room temperature. The absorbances of the MBP sample and the reference sample at the excitation wavelength were adjusted to 0.5.

3. General Principle of the Measurement

In this section, we present a basic theoretical treatment of the measurement of ΔH and ΔV for a simple reversible reaction (one reactant (R) and one product (P)).

$$\mathrm{R} \underset{k_{\mathrm{back}}}{\overset{h\nu}{\rightleftharpoons}} \mathrm{P}$$

Application of this method to a more specific reaction system (photoenolization of MBP) is described in following sections. If the absorptive contribution is negligible and the diffraction efficiency of the probe light is small, the TG signal intensity is proportional to the square of the peak−null difference of the refractive index in the grating pattern. Generally, there are many origins of the refractive index change upon photoirradiation to a matter, but they may be decomposed into four dominant terms under our experimental conditions (isotropic liquid sample excited at a resonant wavelength under a rather weak laser power) as follows.

$$I_{\mathrm{TG}}(t) = A|\delta n_{\mathrm{Q}}(t) + \delta n_{\mathrm{H}}(t) + \delta n_{\mathrm{P}}(t) + \delta n_{\mathrm{V}}(t)|^2 \qquad (1)$$

where A is a constant which represents the sensitivity of the system, δn_{Q} represents the thermal grating due to the nonradiative transition from the initially created excited state to the intermediate states or product P (e.g., *cis*- and *trans*-enols) (Scheme 1), and δn_{H} is originated from the enthalpy change by a chemical reaction. The δn_{P} and δn_{V} terms represent the refractive index changes by the presence of reaction products and depletion of the reactant, and they are sometimes called the "population grating" or "species grating". In this paper, we use the name of "species grating" for describing these contributions and "population grating" is reserved for another contribution. The species grating may be separated into two contributions: One is from the refractive index change which concomitant with the change of absorption bands ($\delta n_{\mathrm{P}}(t)$, the population grating) and the other is due to the molecular volume change ($\delta n_{\mathrm{V}}(t)$, the volume grating). In the latter contribution, the intrinsic molecular volume change as well as the effect of solvent reorganization is contained.

We assume that the thermal energy to create the product P (the first term δn_{Q}) released promptly after the excitation. The time profile can be calculated by solving Fourier's thermal diffusion equation and is given by

$$\delta n_{\mathrm{Q}}(t) = (\mathrm{d}n/\mathrm{d}T)(NQ_{\mathrm{f}}W/\rho C_{\mathrm{p}}) \exp(-D_{\mathrm{th}}q^2t) \qquad (2)$$

where dn/dT is the refractive index change by the temperature change, N the molar density of the excited molecule (mol/cm^3), Q_{f} the thermal energy released by the nonradiative transition (J/mol), ρ density (g/cm^3), W molecular weight (g/mol), C_p heat capacity (J/(K mol)), D_{th} thermal diffusivity (m^2/s), and q magnitude of the grating vector (m^{-1}). It is not difficult to incorporate the time evolution of heat releasing due to a finite rate of the nonradiative transition in this equation. On the other hand, the thermal grating signal due to the enthalpy change (P $\rightarrow$ R) is assumed to be evoluted in the observation time window by the chemical reaction and also by the thermal diffusion. The profile can be expressed by

$$\delta n_{\mathrm{H}}(t) = ((\mathrm{d}n/\mathrm{d}T)WN/\rho C_p)\{\phi\Delta H'(t)^* \exp(-D_{\mathrm{th}}q^2t)\} \qquad (3)$$

where $\Delta H'(t)$ is the time derivative of the heat releasing by the enthalpy change, ϕ is the quantum yield of the reaction, and * represents the convolution. For example, if the reaction process (P $\rightarrow$ R) can be expressed by a single-exponential function with

a rate constant k_{back}, $\Delta H'(t)$ is given by

$$\Delta H'(t) = -\Delta H k_{back} \exp(-k_{back} t) \quad (4)$$

where ΔH is the reaction enthalpy change.

The time profile of the species grating signal is given by Fick's diffusion equation coupled with the chemical reaction. For a reversible reaction, the following equation may be derived.[20]

$$\delta n(q,t) = \delta n_1 \exp(-D_r q^2 t) + \delta n_2 \exp(-(D_p q^2 + k_{back})t) \quad (5)$$

The preexponential factors are given by

$$\delta n_1 = -\delta n_r (D_p q^2 - D_r q^2)/(D_p q^2 - D_r q^2 + k_{back}) \quad (6a)$$

$$\delta n_2 = \delta n_p - (\delta n_r k_{back}/(D_p q^2 - D_r q^2 + k_{back})) \quad (6b)$$

where δn_r and δn_p represent the refractive index change by the presence of the product and the reactant, respectively. D_p and D_r are the diffusion constants of the product and reactant, respectively. δn_r and δn_p contain the population contribution (δn^p) and the volume effect as

$$\delta n_i = N\phi(\delta n_i^p + B\Delta V'_i) \quad (i = \text{P or R}) \quad (7)$$

where $B = V\partial n/\partial V$ (refractive index change by the molecular volume change), and $\Delta V'_i$ is the volume effect by the presence of the species i instead of the solvent molecule.[8] (The reaction volume change (ΔV) is given by $\Delta V = \Delta V'_P - \Delta V'_R$).

Separation of these four contributions in the TG signal consists of two steps.[8] First, the thermal contribution, δn_Q, can be separated from the species grating component by the time-resolved manner. Since the decay rate due to the thermal diffusion ($D_{th}q^2$) is normally 1 or 2 orders of magnitude faster than that of the species grating ($D_p q^2$ or $D_r q^2$), these contributions can be easily separated. Comparing the intensity of the pure thermal grating signal (Q_f) with that of a reference sample, which converts the absorbed photon energy ($h\nu_{ex}$) to the thermal energy with a known efficiency, one can determine $\Delta H\phi$ from a relation of $Q_f + \Delta H\phi = h\nu_{ex}$ in the case of the reversible reaction. (Even if the product does not return back to the reactant, $\Delta H\phi$ can be determined from the TG intensities in the case that Q_f and $\Delta H\phi$ can be separated by the time-resolved measurement.)

Next, the magnitude of the pressure wave from the photoirradiated region is measured. The detection method can be either the PA or the TG techniques. For the TG method, the crossing angle of two excitation beams should be adjusted so that the oscillating acoustic wave should be separated from the diffusive contribution of the thermal grating. The distinction should not be difficult because of the characteristic oscillating feature. For the PA detection, the pressure wave is detected by a pressure-sensitive device such as a piezoelectric transducer. The magnitude of the pressure wave (or the square root of the acoustic TG signal) is proportional to the density change of the matrix through the thermal effect and volume effect. If the time window of the pressure measurement is in a faster region than that of the back reaction P → R (that is, if the enthalpy energy is stored in chemical system), the acoustic intensity by the PA method, I_{ac}, is given by

$$I_{ac} = A'N|Q_f W\alpha_{th}/\rho C_p + \Delta V\phi| \quad (8)$$

where A' is a proportional constant, which includes the sensitivity of the apparatus, and α_{th} is the thermal expansion coefficient. Therefore, comparing the acoustic signal intensity from the sample with that from the reference sample, $\Delta V\phi$ can be determined, because Q_f is already known from the TG measurement.

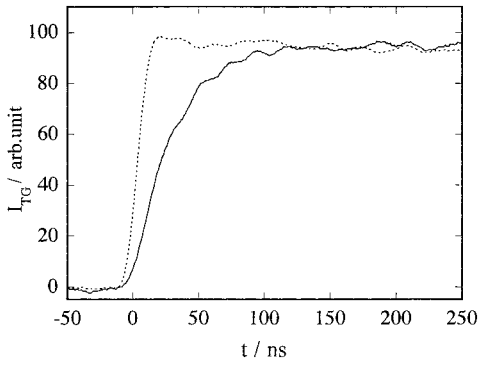

Figure 1. Time profiles of the TG signal after photoexcitation of 2-methylbenzophenone (solid line) and nitrobenzene (dotted line) in a fast time scale. The intensities of the signals are normalized at around 200 ns.

This method was first demonstrated for a photodissociation reaction of DPCP,[8,12] which completes just after the photoexcitation. In this report, we extend this method to a more complex system; a chemical reaction proceeds during the time window with two intermediate species.

4. Results and Discussion

4.1. Time profiles of the TG Signal. First, we describe the TG signal of a reference sample, nitrobenzene in ethanol. After the photoexcitation of nitrobenzene, the TG signal rises within the excitation laser pulse (10 ns), and it decays to the baseline with a time constant of $2D_{th}q^2$. Apparently, the signal is attributed to the thermal grating. The fast rise of the signal is consistent with the fast relaxation from the excited states (excited singlet and triplet states) as reported recently.[21] Since the radiative transition of nitrobenzene is negligible, the signal intensity reflects the temperature rise by the absorbed photon energy ($h\nu_{ex}$).

The TG signals from MBP in ethanol are depicted in Figure 1∼ 3 in several different time scales at $q^2 = 0.21 \times 10^{12}$ m^{-2} and $q^2 = 10.2 \times 10^{12}$ m^{-2}. The signal rises with slower time constants than the instrumental response in a tens of nanoseconds range (Figure 1). The slower rise may represent the decay of the biradical (Scheme 1). The analysis of this component is beyond the scope of this paper and we treat this rise component as a "fast" rise signal (δn_Q component). The temporal features after 100 ns depend on the magnitude of q. For a rather small q (such as $q^2 = 0.21 \times 10^{12}$ m^{-2}), the grating signal further rises slowly in a microsecond time scale (Figure 2a). Then, the signal decays to the baseline once and shows a growth−decay curve (Figure 2b−d). For a larger q (for example, $q^2 = 10.2 \times 10^{12}$ m^{-2}) (Figure 3), the TG signal does not show slow rise but directly decays to the baseline. After that, it rises followed by decays with two different rates: in a few microseconds and in hundreds of microseconds range. These features can be consistently explained by the contributions of the thermal grating and two species gratings. In the following, first, the feature of the grating signal is qualitatively explained and then the profile is analyzed quantitatively in the next section.

The fastest decay component (main signal in Figure 2a and Figure 3a) should be attributed to the thermal grating, which is created by the nonradiative transition to the ground states of

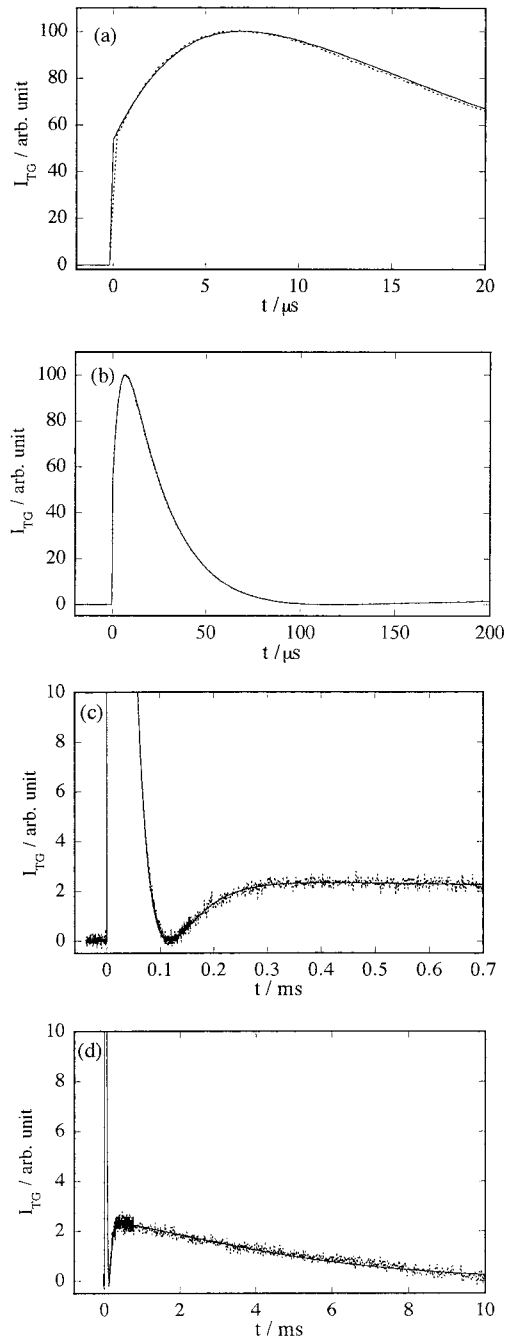

Figure 2. Time profiles of the TG signal (dotted line) after photoexcitation of 2-methylbenzophenone in ethanol and the fitted curve (solid line) in various time scale at $q^2 = 0.21 \times 10^{12}$ m^{-2}.

two enol species via the biradical states, because the decay rate is close to $2D_{th}q^2$ as expected from eq 2. The successive TG signal is due to the species grating of the cis and trans enol forms. The relatively large intensity of this component apparently indicates that the thermal lens signal reported previously[17] should be analyzed including this effect. Since the absorption bands of all species in this reaction system are on the blue side from the probe wavelength (633 nm), the observed signal must consist of the phase grating.

The different feature at different q can be explained by the different lifetime of the thermal grating at different q. When the decay of the thermal grating is slower than the decay of the *cis*-enol, the increase of the thermal energy by the *cis*-enol decay (ΔH effect) as well as the decrease of the species grating results in a rise signal on the thermal grating signal. (Since δn_Q is

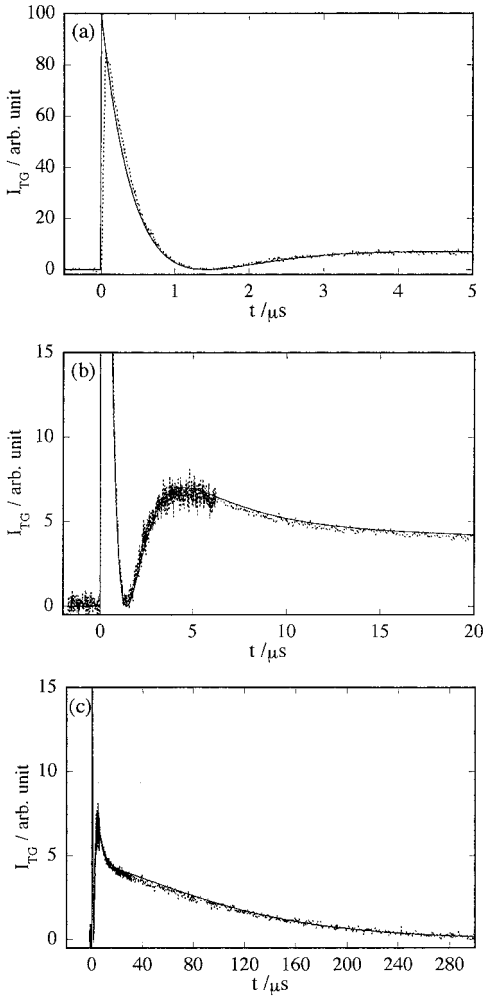

Figure 3. Time profiles of the TG signal (dotted line) and the fitted curve (solid line) in various time scale at $q^2 = 10.2 \times 10^{12}$ m^{-2}.

negative, one can easily find that $\delta n_H + \delta n_P + \delta n_V$ of the *cis*-enol should be negative from the profile.) On the other hand, when the lifetime of the thermal grating signal is shorter than that of the *cis*-enol, the decrease of the species grating contribution appears as the decay of the signal. (The dip between the thermal grating and the species grating signals indicates that $\delta n_H + \delta n_P + \delta n_V$ of the *cis*-enol should be positive at this q. The positive sign of this species grating at larger q results from a smaller contribution of the thermal effect by the convolutional effect.) This different feature at different q is useful for a quantitative analysis as described in the next section. The signal in a longer time scale (after the decay of the thermal grating and the species grating due to the *cis*-enol) represents the diffusion process of the keto and the *trans*-enol.

The acoustic signal can be measured by either the TG method or the PA technique. Although we used the TG method with a small crossing angle of the excitation beams for the acoustic detection previously,[8,12] we found that the PA method provides more stable results than the TG method, probably because of the simpler experimental configuration. Here, the PZT is used for the pressure wave detection. The observed PA signal of MBP is much weaker than that of the reference (nitrobenzene) sample (Figure 4).

4.2. Analysis of the TG Signal. The observed TG signal should be fitted by eq 1. However, in this case, since two products (*cis*- and *trans*-enols) and the reactant (the keto form) participate in the signal, the original eqs 1−7 should be modified as follows. First, for the thermal contributions, eq 3 should be

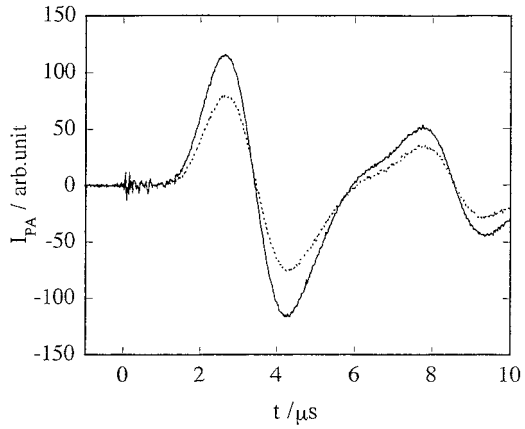

Figure 4. PA signal of 2-methylbenzophenone (dotted line) and nitrobenzene (solid line).

rewritten as

$$\delta n_H(t) = ((dn/dT)NW/\rho C_p)[\{\phi_c \Delta H_c'(t)*\exp(-D_{th}q^2t)\} + \{\phi_t \Delta H_t'(t)*\exp(-D_{th}q^2t)\}] \quad (9)$$

where $\Delta H_c(t)$ and $\Delta H_t(t)$ are given by

$$\Delta H_c(t) = \Delta H_c \exp(-k_c t)$$

$$\Delta H_t(t) = \Delta H_t \exp(-k_t t) \quad (10)$$

and ϕ, ΔH, and k represent the quantum yield of the production, enthalpy change, and the decay rate constant, respectively, and the subscripts of c and t indicate the *cis*- and *trans*-enols.

Next, for the species grating, the back reaction from the *cis*-enol to keto form ($k_c \approx 4$ μs) is much faster than the mass diffusion time ($D_c q^2$ or $D_t q^2$ are in the order of 100 μs or longer). Hence, from eq 5, the time dependence of the species grating signal due to the *cis*-enol can be written as

$$\delta n_c(t) = (\delta n_c - \delta n_k) \exp(-k_c t) \quad (11)$$

where δn_c and δn_k are the refractive index changes by the *cis*-enol and keto forms, respectively. On the other hand, since the intrinsic lifetime is much longer than the diffusion rate for the *trans*-enol ($k_t = 10-172$ s$^{-1} \ll D_c q^2$ or $D_t q^2$), species grating due to the *trans*-enol (eq 5) can be reduced to

$$\delta n_t(t) = -\delta n_k \exp(-D_k q^2 t) + \delta n_t \exp(-(D_t q^2 + k_t)t) \quad (12)$$

where δn_t represents the refractive index changes by the *trans*-enol, and D_k and D_t are the diffusion constants of the keto and *trans*-enol, respectively.

As described in the previous section, δn_c, δn_t, and δn_k can be decomposed into the population and volume contributions.

$$\delta n_c = N\phi_c(\delta n_c^{\,p} + B\Delta V'_c)$$

$$\delta n_t = N\phi_t(\delta n_t^{\,p} + B\Delta V'_t)$$

$$\delta n_k = N\phi(\delta n_k^{\,p} + B\Delta V'_k) \quad (13)$$

where $\delta n_c^{\,p}$, $\delta n_t^{\,p}$, and $\delta n_r^{\,p}$ denote the population grating contributions in the corresponding species grating, $\Delta V'$ has the same meaning as that in eq 7, and $\phi = \phi_c + \phi_t$. The reaction volume change of the *cis*- (ΔV_c) and *trans*-enols (ΔV_t) are given by $\Delta V_c = \Delta V'_c - \Delta V'_k$ and $\Delta V_t = \Delta V'_t - \Delta V'_k$, respectively.

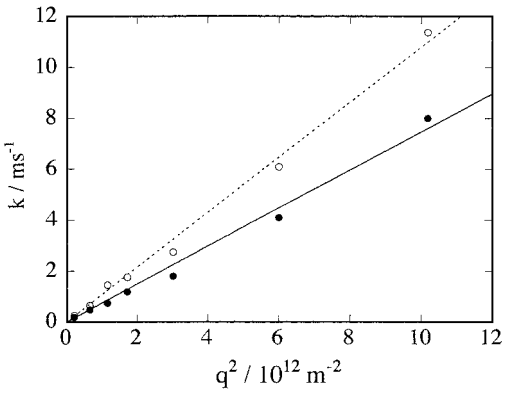

Figure 5. Plots of the decay rate constants (k) against q^2 for the keto form (open circles) and *trans*-enol form (closed circles).

The time profile in a longer time scale than $(D_{th}q^2)^{-1}$ or k_c^{-1} can be expressed well by a biexponential function.

$$I_{TG}(t)^{1/2} = |a_f \exp(-k_f t) + a_s \exp(-k_s t)| \quad (14)$$

where subscripts f and s stand for the fast and slow components, respectively. From the feature of the grating signal, it is apparent that the sign of the preexponential factor is opposite and, from a comparison with the sign of the thermal contribution (δn_Q and $\delta n_H < 0$), one may find $a_f < 0$ and $a_s > 0$. These two contributions should be due to the species grating of the keto and *cis*-enol forms. From the Kramers−Kronig relation ($\delta n_k^{\,p} > 0$, $\delta n_t^{\,p} > 0$) and eq 12, the faster and slower components are assigned to the keto and *trans*-enol, respectively; that is, $k_f = D_k q^2$ and $k_s = D_t q^2 + k_t$. The profile can be fitted accurately by the least-squares method, and the rate constants, k_f and k_s, are plotted against q^2 in Figure 5. The plot shows that k_f is proportional to q^2 with an intercept $k_f = 0$ at $q^2 = 0$. The q^2 dependence of k_s is also linear but it has an finite intercept $k_s \approx 10$ s^{-1} at $q^2 = 0$. From the slopes, diffusion constants of the keto and *trans*-enol forms are determined as $D_k = 1.0 \times 10^{-9}$ m^2 s^{-1} and $D_t = 0.70 \times 10^{-9}$ m^2 s^{-1}. The intercept of the slow component represents the intrinsic lifetime of the *trans*-enol.

At first glance, one may think that there are too many parameters (Q_f, ΔV_c, ΔV_t, ΔH_c, ΔH_t, D_{th}, D_t, D_c, k_c, k_t, ϕ_c, ϕ_t, δn_k, δn_c, and δn_t) to be uniquely determined from the curve fitting of the TG signal. However, some of them are already known from previous studies and most of them can be evaluated one by one from the TG and PA signals.

(i) First, some rate constants are rather easily determined from the temporal profiles. For example, the decay rate of the thermal grating, $D_{th}q$,^{2} is uniquely determined by a single-exponential fit of the TG signal from the reference sample.

(ii) The slow rise of the TG signal under a condition of $k_c \gg D_{th}q^2$ or the thermal lens condition represents the decay rate of the *cis*-enol, k_c. The lifetime of the *trans*-enol, k_t^{-1}, is easily evaluated from the transient absorption or the q^2 plot of $D_t q^2 + k_t$. The value, 10 s^{-1}, is smaller than the previously reported value (172 s^{-1}). However, this discrepancy in the lifetime is not serious for the determination of the other quantities, such as ΔH and ΔV, because our signal observation time range is sufficiently shorter than this time, and the ΔH_t contribution in the signal is negligibly small due to the convolutional effect. Actually we obtain very similar values either using $k_t = 10$ s^{-1} or $k_t = 172$ s^{-1}.

(iii) For simplicity, we assume that $\Delta V'_c$ is the same as $\Delta V'_t$; in other words, ΔV is the same both for the *cis*- and *trans*-

TABLE 1: Physical Properties of the Photoenolization of MBP

$D_t/10^{-9}$ m^2 s^{-1}	0.7 ± 0.1
$D_k/10^{-9}$ m^2 s^{-1}	1.0 ± 0.1
$k_t/10$ s^{-1}	1.0 ± 0.5[a]
$k_c/10^6$ s^{-1}	2.5 ± 0.1[b]
Q_f/kJ mol^{-1}	239 ± 20
$\phi_t\Delta H_t$/kJ mol^{-1}	44 ± 4
$\phi_c\Delta H_c$/kJ mol^{-1}	54 ± 5
$\phi_t\Delta n_t$	0.27 ± 0.03[c]
$\phi_c\Delta n_c$	0.44 ± 0.05[c]
$\phi\Delta n_p$	0.46 ± 0.05[c]
ΔV/cm^3 mol^{-1}	-12 ± 5

[a] Determined from the q^2 plot of the decay rate constants of the TG signal. [b] Measured by the transient absorption method. [c] Normalized by the thermal contribution ($\delta n_Q + \delta n_H = 1$).

enols ($\Delta V \equiv \Delta V_c = \Delta V_t$). This assumption may not be exactly correct. For example, we already know that the *cis*-azobenzene is slightly smaller than the trans form.[1,2] However, contrary to azobenzene, the difference in structure between the *cis*- and *trans*-enols is not drastic for this molecule. We think that this small different volume between the *cis*- and *trans*-enols can be neglected compared with the volume change associated with the chemical reaction from the keto to enol forms.

(iv) The decay in the longer time scale than $1/k_c$ or $1/D_{th}q^2$ reflects the translational diffusion of the keto and *trans*-enol forms. By the least-squares fit by a biexponential function (eq 14), D_kq^2 and $D_tq^2 + k_t$ can be accurately determined. The relative intensities of the preexponential factors are given by δn_k:δn_t.

(v) The TG intensity just after the excitation (but long enough for the decay of the biradicals) can be easily measured accurately and this quantity is proportional to $\delta n_Q(0) + \delta n_c(0) + \delta n_t(0) - \delta n_r(0)$.

(vi) The species grating intensity extrapolated to $t \sim 0$ gives $\delta n_t(0) + \delta n_c(0) - \delta n_k(0)$. Subtracting the species grating intensity from the total intensity at $t = 0$ ($\delta n_Q(0) + \delta n_t(0) + \delta n_c(0) - \delta n_k(0)$) gives δn_Q. By comparison with the intensity from the reference sample, Q_f can be determined.

(vii) The slow rise intensity under a condition of $k_c \gg D_{th}q^2$ (Figure 2) or under the thermal lens condition represents the back reaction from the *cis*-enol to keto, and this intensity is given by $\phi_c\Delta H_c + \delta n_c - \phi_c\delta n_k$. Under the condition of $k_c < D_{th}q^2$ (Figure 3), the thermal contribution from this process becomes small due to the convolutional effect. Therefore, the back reaction appears as the decay of the signal and the intensity is approximately represented as $\delta n_c - \phi_c\delta n_k$. Hence, $\phi_c\Delta H_c$ and $\delta n_c - \phi_c\delta n_k$ can be separately determined. From a relation of $h\nu_{ex} = Q_f + \phi_c\Delta H_c + \phi_t\Delta H_t$, $\phi_t\Delta H_t$ is calculated.

(viii) PA intensity at $t \sim 0$ is given by eq 8. Dividing this intensity by the PA intensity from the reference sample, one obtains $Q_f/h\nu_{ex} + \phi\Delta V\rho C_p/W\alpha_{th}$. Since Q_f is already known from (vi), $\phi\Delta V$ can be evaluated.

(ix) The quantum yield of the reaction is reported to be unity ($\phi = \phi_c + \phi_t = 1.0$).

From these steps, we can determine each quantity uniquely. The determined quantities from the TG and PA signals are summarized in Table 1. Checking the adequacy of these values, we can successfully fit the TG signal in a range of 100 ns to 5 ms at various q's with one set of the parameters. (A slight disagreement between the observed and calculated signal in 0−50 ns is notable (e.g., Figure 3a). This disagreement must be due to the reaction of the biradical. Here the signal in that time scale was neglected in the fitting process.)

4.3. Photoenolization of MBP. In the following sections, the determined quantities are discussed based on the molecular structural change by the photoenolization.

(A) Diffusion Constant. From the q^2 plot of the decay rate constants, D_k and D_t are determined as 1.0×10^{-9} and 0.70×10^{-9} m^2 s^{-1}, respectively. D of benzophenone in ethanol was reported as 0.95×10^{-9} m^2 s^{-1} by the Taylor dispersion method[22] and as 1.0×10^{-9} m^2 s^{-1} by the TG method.[23] D of the keto form agrees well with these values, which indicates almost no effect of the intramolecular hydrogen bonding to D. On the contrary, D of the enol form is much smaller than D of the keto form, which may be explained by the intermolecular hydrogen bonding to the solvents. The additional attractive intermolecular interaction causes a friction during the translational movement. The effect of the intermolecular hydrogen bond of some stable molecules on the diffusion constant has been recently investigated by Chan and Chan[24] and Tominaga et al.[25] using the Taylor dispersion method. D's of solutes which can form the intermolecular hydrogen bond with solvent are reduced considerably from D's of non-hydrogen-bonding solutes. For example, D of cyclohexanone in ethanol is 1.34×10^{-9} m^2 s^{-1}, while D of cyclohexanol is 0.87×10^{-9} m^2 s^{-1} in the same solvent. The ratio of D_k to D_t is comparable to the reported value. The reduction of D by the photoirradiation is clear evidence of the enol formation by the reaction. This photoenolization will allow us to extract the influence of the hydrogen bond to the diffusion process in future.

(B) Population Grating. The determined sign of the population gratings (δn_c^P, δn_t^P, and δn_k^P) is positive, which is consistent with the absorption spectra of these species and the Kramers−Kronig relation. The magnitude of δn_k^P is smaller than the other ones. This relation is also consistent with a prediction from the Kramers−Kronig relation and the position of the absorption bands of each species (the peak of the first absorption band of the enol form is closer to the wavelength of the probe laser than that of the keto form). It is interesting to note that the ratio of $\phi_c\delta n_c$:$\phi_t\delta n_t = 0.62$:0.38 is the same as the branching ratio of the *cis*- and *trans*-enols determined from the quenching experiment.[15] It suggests that δn_c^P is very similar to δn_t^P, which seems reasonable because the absorption spectra of both species resemble each other. While, the branching ratio (ϕ_c:ϕ_t)was reported as 0.7:0.3 from the transient absorption signal under an assumption that the molar extinction coefficient of the *trans*- and *cis*-enols are the same.[17] At present, we cannot conclude which branching ratio is correct. A reliable molecular orbital calculation will be helpful to estimate the molar extinction coefficient of both species.

(C) Molecular Volume Change. The determined ΔV (<0) clearly shows that the molecular volume is reduced by transformation from the keto to the enol forms. The reaction volume change could be divided into two contributions: one is the intrinsic volume change, which is due to changes in bond lengths and angles, and the other is the external volume, which may contain two contributions: a void volume change associated with the solute molecular structure and the electrostriction with solvent. The van der Waals volume of the keto and enol forms may be calculated by an atom increment method proposed by Bondis.[26] If we define this as the intrinsic volume, the intrinsic volume change by the isomerization is calculated to be only -0.7 cm^3/mol. The observed volume change must come from other sources.

The intermolecular hydrogen bond could contribute to ΔV, because the creation of the hydrogen bond should significantly alter the solvation structure around the solute. Although the

effect of the hydrogen bond to molecular volume is not well elucidated, it is expected that the attractive interaction with the solvent contract the volume by the creation of the hydrogen bond. Ikawa and co-workers have measured the volume change by breaking intramolecular hydrogen bond using the pressure dependence of the IR absorption bands.[27] They found that the volume is contracted about 4 cm^3/mol by the interaction of the hydroxy group with solvent (CCl_4). This value was reasonably accounted for by an electrostriciton effect with the solvents.[27] Considering the much polar character of ethanol, one would not be surprised to find that the observed volume change in the keto−enol reaction (−12 cm^3/mol) is explained by the external volume changes associated with the intermolecular hydrogen bonding.

(D) Enthalpy Changes. Recently Suzuki et al. determined the heat of formation of *cis*- and *trans*-enols using the TL techniques as 116 and 202 kJ/mol, respectively.[17] However, the TL signal was analyzed only from the thermal energy even though the probe wavelength is the same as in this study (He−Ne laser). Considering the relatively large contributions of the ΔV and population grating in the TG signal, these contributions should be included in the TL analysis, too. Our determined ΔH of the *trans*- and *cis*-enols are smaller than their values and the difference between these reports should be attributed to the neglection of the population lens and ΔV contributions in the TL analysis. One of the methods to evaluate these contributions in the TL signal was presented previously using the solvent variation.[8] However, a similar technique cannot be used for this system because the photoenolization reaction itself is sensitive to the matrix. As far as we know, this time-resolved TG technique is the only way to perform the quantitative measurement. If we calculate the heats of reaction of the *cis*- and *trans*-enols with $\phi_c = 0.62$, and $\phi_t = 0.38$, $\Delta H_c = 87$ kJ/mol and $\Delta H_t = 115$ kJ/mol ($\Delta H_t - \Delta H_c = 28$ kJ/mol) are obtained. If we use $\phi_c = 0.7$, and $\phi_t = 0.3$, $\Delta H_c = 77$ kJ/mol and $\Delta H_t = 146$ kJ/mol ($\Delta H_t - \Delta H_c = 69$ kJ/mol) are obtained. This energy difference could be due to the steric hindrance between the phenyl and vinyl groups for the *trans*- and *cis*-enols as suggested by Suzuki et al.;[17] however, the enthalpy difference should be smaller than that they have reported.

5. Summary

Various contributions in the TG signal observed upon the photoenolization of 2-methylbenzophenone were separated by the time-resolved technique. They are the thermal contribution by the nonradiative transition among the excited states, enthalpy change (ΔH) and volume change (ΔV) by the keto−enol photoconversion, and population grating which is associated with the absorption spectrum change by the reaction. Comparing with the TG intensity of a reference sample, these quantities are determined simultaneously without changing any external properties such as solvents, pressure, and temperature. The slower diffusion constant and smaller molecular volume of the enol form are attributed to the intermolecular hydrogen bonding. The relative magnitudes of the population gratings are consistent with the absorption spectra of these species and also the branching ratio between the *cis*- and *trans*-enol forms. We should emphasize that this reaction system is not a special case that these various origins contribute to the signal simultaneously. Generally we should take into account these contributions whenever the photophysical processes are studied by the TL or TG methods.

Acknowledgment. I am indebted to Prof. N. Hirota in Kyoto University for his discussion and encouragement. I also acknowledge Dr. T. Suzuki and Prof. T. Ichimura in Tokyo Institute of Technology for their helpful discussions.

References and Notes

(1) Asano, T.; le Noble, W. J. *Chem. Rev.* **1978**, *78*, 407.
(2) VanEldik, R.; Asano, T.; le Noble, W. J. *Chem. Rev.* **1989**, *89*, 549.
(3) Okamoto, M.; Teranishi, H. *J. Am. Chem. Soc.* **1986**, *108*, 6378.
(4) Bonetti, G.; Vecli, A.; Viappiani, C. *Chem. Phys. Lett.* **1997**, *269*, 268.
(5) Hung, R. R.; Grobowski, J. J. *J. Am. Chem. Soc.* **1992**, *114*, 351.
(6) Herman, M. S.; Goodman, J.L. *J. Am. Chem. Soc.* **1989**, *111*, 1849. Westrick, J. A.; Goodman, J.L.; Peters, K.S. Biochemistry **1987**, *26*, 8318. Herman, M. S.; Goodman, J. L. *J. Am. Chem. Soc.* **1989**, *111*, 9105.
(7) Marr, K.; Peters, K. S. *Biochemistry* **1991**, *30*, 1254. Malkin, S.; Churio, M. S.; Shochat, S.; Braslavsky, S. E. *J. Photochem. Photobiol.* **1994**, *23B*, 79.
(8) Hara, T.; Hirota, N.; Terazima, M. *J. Phys. Chem.* **1996**, *100*, 10194.
(9) Schulenberg, P. J.; Gartner, W.; Braslavsky, S. E. *J. Phys. Chem.* **1995**, *99*, 961.
(10) Zimmt, M. D. *Chem. Phys. Lett.* **1989**, *160*, 564. Ma, J.; Dutt, G. B.; Waldeck, D. H.; Zimmt, M. B. *J. Am. Chem. Soc.* **1994**, *116*, 10619.
(11) Morais, J.; Ma, J.; Zimmt, M. B. *J. Phys. Chem.* **1991**, *95*, 3885. Morais, J.; Zimmt, M. B. *J. Phys. Chem.* **1995**, *99*, 8863.
(12) Terazima, M.; Hara, T.; Hirota, N. *Chem. Phys. Lett.* **1995**, *246*, 577.
(13) Yamaguchi, S.; Hirota, N.; Terazima, M., to be submitted for publication.
(14) Yamaguchi, S.; Hirota, N.; Terazima, M., unpublished work.
(15) Sammes, P. G. *Tetrahedron* **1976**, *32*, 405.
(16) Das, P. K.; Encinas, M. V.; Small Jr., R. D.; Scaiano, J. C. *J. Am. Chem. Soc.* **1979**, *101*, 6965. Nakayama, T.; Hamanoue, K.; Hidaka, T.; Okamoto, M.; Teranishi, H. *J. Photochem.* **1984**, *24*, 71.
(17) Suzuki, T.; Okuyama, U.; Ichimura, T. *Chem. Phys. Lett.* **1997**, *266*, 107.
(18) Terazima, M.; Hirota, N. *J. Chem. Phys.* **1993**, *98*, 6257.
(19) Terazima, M.; Azumi, T. *Bull. Chem. Soc. Jpn.* **1989**, *62*, 2862.
(20) Terazima, M.; Okamoto, K.; Hirota, N. *J. Phys. Chem.* **1993**, *97*, 5188.
(21) Takezaki, M.; Hirota, N.; Terazima, M. *J. Phys. Chem. A* **1997**, *101*, 3443.
(22) Donkers, R. L.; Leaist, D. G. *J. Phys. Chem. B* **1997**, *101*, 304.
(23) Terazima, M.; Okamoto, K.; Hirota, N. *J. Phys. Chem.* **1995**, *97*, 13387. Okamoto, K.; Hirota, N.; Terazima, M. *J. Phys. Chem.*, in press.
(24) Chan, M. L.; Chan, T. C. *J. Phys. Chem.* **1995**, *99*, 5765.
(25) Tominaga, T.; Tenma, S.; Watanabe, H. *J. Chem. Soc. Faraday Trans.* **1996**, *92*, 1863.
(26) Edward, J. T. *J. Chem. Educ.* **1970**, *47*, 261.
(27) Kamiya, N.; Sekigawa, T.; Ikawa, S. *J. Chem. Soc., Faraday Trans.* **1993**, *89*, 489. Cho, T.; Kida, I.; Ninimiya, J.; Ikawa, S. *J. Chem. Soc., Faraday Trans.* **1994**, *90*, 103. OkuyamaM.; Ikawa, S. *J. Chem. Soc., Faraday Trans.* **1994**, *90*, 3065.